$$X_1 = \frac{3\Gamma R_G TI \sum d_i^2 P(d_i) t}{PFa \sum_i d_i^3 P(d_i)} = k_0 t \qquad (21)$$

where

$$k_0 = \frac{3\Gamma R_G TI \sum_i d_i^2 P(d_i)}{PFa \sum_i d_i^3 P(d_i)}$$

The amount of CTAB adsorbed by latex particles is also calculated as:

$$X_2 = \Gamma \pi d_p^2 n_p V_s \qquad (22)$$

After all, the time required for the amount of CTAB to decrease by 10% of initial concentration is given as:

$$X_1 + X_2 = 0.1 \times C' V_s \qquad (23)$$

$$t = \frac{0.1 C' V_s - X_2}{K_0} \qquad (24)$$

LITERATURE CITED

Anfruns, J. F., and J. A. Kitchner, "Rate of Capture of Small Particles in Flotation," *Trans. Inst. Min. Metall.*, **86**, C9 (1977).

Brenner, H., "The Slow Motion of a Sphere through a Viscous Fluid towards a Plane Surface," *Chem. Eng. Sci.*, **16**, 242 (1961).

Collins, G. L., and G. J. Jameson, "Experiments on the Flotation of Fine Particles," *Chem. Eng. Sci.*, **31**, 985 (1976).

Collins, G. L., and G. J. Jameson, "Double-layer Effects in the Flotation of Fine Particles," *Chem. Eng. Sci.*, **32**, 239 (1977).

Collins, G. L., M. Motarjemi, and G. J. Jameson, "A Method for Measuring the Charge on Small Gas Bubbles," *J. Colloid Interface Sci.*, **63**, 69 (1978).

Flint, L. R., and W. J. Howarth, "The Collision Efficiency of Small Particles with Spherical Air Bubbles," *Chem. Eng. Sci.*, **26**, 1155 (1971).

Fukui, Y., and S. Yuu, "Collection of Submicron Particles in Electroflotation," *Chem. Eng. Sci.*, **35**, 1097 (1980).

Fukui, Y., and S. Yuu, "Measurement of the Charge on Small Gas Bubble," *AIChE J.* (Nov., 1982).

Higashitani, K., T. Tanaka, and Y. Matsuno, "A Kinematic Interpretation on Coagulation Mechanism of Hydrophobic Colloids," *J. Colloid Interface Sci.*, **63**, 551 (1978).

Honig, E. P., G. J. Roebersen, and P. H. Wiersema, "Effect of Hydrodynamic Interaction of the Coagulation Rate of Hydrophobic Colloids," *J. Colloid Interface Sci.*, **36**, 97 (1971).

Jameson, G. J., S. Nam and M. Moo Young, "Physical Factors Affecting Recovery Rates in Flotation," Minerals Sci. Engng., **9**, 103 (1977).

Lyklema, J., "Principles of the Stability of Lyophobic Colloidal Dispersions in Nonaqueous Media," *Adv. Colloid Interface Sci.*, **2**, 65 (1968).

Pethica, B. A., "The Adsorption of Surface Active Electrolytes at the Air/Water Interface," *Trans. Faraday Soc.*, **60**, 413 (1954).

Reay, D., and G. A. Ratcliff, "Removal of Fine Particles from Water by Dispersed Air Flotation: Effects of Bubble Size and Particle Size on Collection Efficiency," *Can. J. Chem. Eng.*, **51**, 178 (1973).

Reay, D., and G. A. Ratcliff, "Experimental Testing of the Hydrodynamic Collision Model of Fine Particle Flotation," *Can. J. Chem. Eng.*, **53**, 481 (1975).

Siegerman, H., "Applications of Electrochemistry to Environmental Problems," *Chem. Tech.*, **11**, 673 (1971).

Yuu, S., and Y. Fukui, "Measurement of Fluid Resistance Correction Factor for a Sphere Moving through a Viscous Fluid toward a Plane Surface," *AIChE J.*, **27**, 168 (1981).

Manuscript received July 14, 1982; revision received October 28 and accepted November 11, 1983.

Two-Component Laser Doppler Velocimeter Studies of Submerged Jets of Dilute Polymer Solutions

Axisymmetric submerged jets of dilute solutions of poly(ethylene oxide) and polyacrylamide of high molecular weight were studied using a two-component laser Doppler velocimeter. At from 40–60 jet diameters from the source the small eddies are suppressed in the solutions studied. The behavior of the large eddies depends upon the elastic nature of the solution.

N. S. BERMAN and HUNG TAN

Department of Chemical and Bio Engineering
Arizona State University
Tempe, AZ 85287

SCOPE

Submerged jets are an important way to obtain mixing in engineering practice and are also an important experimental arrangement for the study of mixing. For Newtonian fluids the large scale structure of turbulent jets does not depend upon viscosity. Experimental measurements with dilute polymer solutions in submerged jets show that the jet is unaffected by the polymers in some cases (Barker, 1973) and is drastically changed in other cases (Usui and Sano, 1980a). Photographs of jets containing fibers or polymer solutions show large reductions in turbulent mixing and sharp well-defined boundaries between the ambient fluid and the fluid which came out of the jet. These previous studies were imprecise or qualitative but they do suggest that the inviscid character of the jet is sometimes changed.

In the present work we investigate the effect of molecular expansion in the initial preparation of the polymer solution on the details of the turbulent fluctuations. Polyethylene oxide (PEO) and polyacrylamide (PAM) were dissolved in waters of different purity to change the expansion of the molecules. Flow visualization of the dyed jet and laser Doppler velocity (LDV) measurements of the velocity fluctuations in the axial and radial directions were used to observe the differences in turbulent mixing.

CONCLUSIONS AND SIGNIFICANCE

Studies of the flow structure of submerged jets containing polymer additives show that the polymers can affect both the large-scale and the small-scale structure of the jet. The influence on the large scale depends on the formation of coherent elastic threads which are large enough to interact with the turbulence. Small diameter threads oscillate or break up in the flow to create increased longitudinal fluctuations compared to the turbulent fluctuations in a Newtonian jet. If the threads are thick enough, oscillations are suppressed and the spread of the jet in the radial direction is reduced. In either case the small eddies in the flow are suppressed and turbulent diffusion is reduced.

Molecular expansion in high purity water increased the effects of the polymers. For 100 ppm PAM in deionized water the jet was laminar with instabilities along the interface with the ambient polymer solution. The evidence points to the existence of networks of polymers and associated solvent. These networks can be broken to give particles larger than the turbulent microscale which inhibit mixing. We conclude that the elasticity of a polymer solution does have an effect on jet mixing.

INTRODUCTION

The details of turbulent mixing in dilute polymer solutions are important in industrial processes and in theoretical studies. A submerged jet is a convenient experimental apparatus for the analysis of mixing. Previous studies of dilute polymer solutions in submerged jets have shown unusual variations.

Two recent studies of dilute polymer solutions in submerged jets utilized optical methods which do not disturb the flow (Barker, 1973; Usui and Sano, 1980a,b). Barker used a one-component laser Doppler velocimeter to measure axial velocity profiles and axial turbulence intensity at the center of a 6.2 mm jet as a function of downstream distance from the jet. He used 50 and 100 ppm solutions of a high molecular weight polyethylene oxide, POLYOX WSR 301. The maximum jet constriction strain rate used by Barker was only 540 s^{-1}, which may be below the strain rate necessary to elongate individual polymer molecules. Barker found no effect of polymers compared to water unless the jet initial condition was the exit of a turbulent pipe flow. In these cases Barker found that the axial turbulence intensity at the jet center was higher for the polymer solution than for pure water and the spreading rate was increased for the polymer solution. The center-line velocity was lower for the polymer solution for x/d between 8 and 47. The nozzle of the jet in Barker's experiments had a 30:1 area ratio. Barker's maximum value of 20% for the turbulent intensity of pure water was less than the 28% found by Wygnanski and Fiedler (1969), because some of the turbulent fluctuations were removed by Barker in his signal processing procedure.

Usui and Sano (1980a,b) used photographic analysis of a small amount of data of the trajectories of 200 μm particles to obtain the velocity and velocity fluctuations in a 10 mm dia. jet of 50 and 200 ppm poly(ethylene oxide) solutions. The molecular weight of the polymer was similar to that of Barker, but the effect on the jet was markedly different. The strain rate at the nozzle exit in the experiments was also low (about 200 s^{-1}). Visualization of the gross structure of the jet and velocity measurements showed that the spreading rate of the polymer solution jets was reduced compared to the spreading rate of the solvent jet. Centerline velocities were higher than for the Newtonian fluid from x/d of 10 to 30. After x/d of 30 the centerline velocities were similar to the Newtonian case. Compared to pure water, the axial turbulent intensity for polymer solutions was higher in the center and decreased more rapidly in the radial direction. Measurements on pure solvent agreed with Wygnanski and Fiedler (1969). Radial intensities and Reynolds stresses were lower for the polymer solutions. Usui and Sano also found increased longitudinal integral scales and increased values of the ratio of the longitudinal to lateral integral scale. Polymer solutions and fiber suspensions gave similar reduced mixing in flow visualization studies by Filipsson et al. (1977).

The polymer solutions used in jet studies are at much higher concentrations than required for drag reduction. There appears to be no way to provide a high strain rate in a jet corresponding to a turbulent boundary layer except in the constriction at the start of the jet. Barker recognized that this initial condition was important and might explain previous different experimental results. One explanation is that the macromolecules stretch in the entrance or boundary layer when the strain rate of the flow multiplied by the molecular time scale is of order one. This seems to correlate with differences observed by Barker, but Usui and Sano found large changes at lower strain rates and the fiber suspensions of Filipsson et al., do not respond to high strain rates in the same way as polymer solutions.

The viscoelastic properties of dilute polymer solutions have been measured in jets by Metzner and Metzner (1970) and in a cone and plate viscometer by Chang and Darby (1983). Hinch and Elata (1979) proposed that the polymer solution properties found in weak flows can be explained by the formation of networks of polymers in the solutions. The present work was designed to make accurate velocity measurements in polymer solution jets and to investigate effects of polymer expansion which might be related to the hypothesis of Hinch and Elata (1979).

EXPERIMENTAL

Polymer Solutions

The polymers used were Union Carbide POLYOX WSR 301, a polyethylene oxide (PEO) with molecular weight about 2-4 $\times$ 10^6, and Betz 1120, a partially hydrolyzed polyacrylamide (PAM) with molecular weight about 10^7. The polymers were mixed to 4,000 ppm batches of 16 liters and allowed to stand for 48 hours. The final dilution to 25 or 100 ppm was made at least two hours before the experimental data were taken. The dilute polymer solutions were used in a once-through system and then discarded. To achieve different molecular expansions in the solutions before they were subject to high strain and high shear, the PEO and PAM were dissolved in waters of different purity. The flow rate through the jet and the viscosity of the polymer solutions were used to monitor the differences between batches of polymer solutions. We consider 100 ppm solutions of the polymers. PEO in tap water had a viscosity 10% higher than the solvent and a flow rate 10% lower. PEO in deionized water had a viscosity 17% higher than the solvent and a flow rate 20% lower. The deionized water was from a university supply of boiler feedwater piped to the laboratory and used as the source of distilled water. PAM in deionized water had a viscosity about twice that of the water and a flow rate 33% lower. When the water was additionally passed through a Barnstead Nanopure deionizer, the PAM

solution viscosity jumped to three times that of water and the jet flow rate dropped slightly to 40% less than the pure water. The viscosities were measured with size 50 and 75 Cannon-Fenske capillary tube viscometers. No significant differences were found whether the viscosity was measured either before or after flowing through the apparatus. Our experiments included polymers in each type of water, so we will call the laboratory tap deionized water, distilled water; and the doubly deionized water, deionized water. The increases in viscosity represent expansion of the polymer molecules in the solutions and this expansion also increases the probability of interaction between molecules.

Jet Constriction and Enclosure

The flow system consisted of a constant head tank connected to a constriction mounted in the center of a 10 cm square transparent box 50 cm long. Both the upper and lower levels were held constant by means of overflow wiers. The 45° cone constriction area ratio was 30.9:1. Following the constriction was a 3 mm length of straight tube 2 mm in diameter. The tube was smooth with no trip and the jet diameter was assumed to be the same as the tube, 2 mm. For flow visualization, india ink in a small amount of polymer solution was injected into the rubber inlet tube leading to the constriction. The water exit flow rate was 14.1 cm^3/s which gave a Reynolds number at room temperature of 10^4 at the constriction exit.

Laser Dopper Velocimeter (LDV)

A Spectra Physics Model 162A-09 air-cooled argon ion laser was used as the light source. The 1 mm dia. beam was expanded to 2.25 mm and then split into four beams. The four beams consisted of two pairs of beams in different polarizations which were focused through a 250 mm lens to a spot in the flow. Another 250 mm lens was used as the receiving optic and the pairs were separated with a polarizing beam splitter. The dual-beam arrangement was used to detect the scattered light from natural seeds in the flows with two EMI 9659B photomultiplier tubes mounted behind 100 μm apertures. There is not sufficient intensity of scattering from polymer molecules to detect the motions of individual molecules or groups of molecules. The location of the optical scattering volume could be measured to within 0.02 mm in the y direction with two dial gages. The x or axial direction along the jet could be changed by moving lab jacks which formed the support for the optics. The focusing optics and laser were mounted on a separate small milling table to provide adjustments in the third direction. For two-component studies each pair of beams was oriented 45° to the mean flow direction and 90° to each other so that the sum of the two Doppler shifts gave $2u$ and their difference gave $2v$. The studies of the variation of mean velocity and axial fluctuations with x were done with a one-component system formed by rotating the optics 45°. The beam intersection is approximately an ellipsoid with diameters based on e^{-2} intensity points of 60 × 600 μm. The shorter axis was in the direction of the jet flow and the larger across the jet. The photomultiplier signals were amplified and sent to two TSI model 1090 trackers. The data were recorded on an Ampex PR-500 FM tape recorder and, since the tape recorder had a high frequency cut off of 1,200 Hz, all frequency spectra were also measured on-line with a Nicolet 440A spectrum analyzer. Most of the other data were also checked both on-line and after tape-recording. The turbulent intensities, Reynolds stress, autocorrelation, and probability were all obtained from a Hewlett Packard 3721A Correlator. Mean velocities were found by averaging the D.C. level from the trackers after taking the sum and the difference. The averaging was done on a Hewlett Packard 5328A universal counter with an integrating voltmeter attachment. Typically, five-minute averages were used.

The mean velocity measurement is independent of the signal amplification within the trackers, however the measured fluctuations are not. The techniques of Berman and Dunning (1973) can be used to find the point at which random phase noise will overwhelm the turbulence. This turns out to be quite low and comparable to instrument noise in our system if the turbulence and noise are uncorrelated. However, the technique used in the TSI tracker tends to correlate all sources of noise with turbulence. This seems to make the noise fall off as a random telegraph signal, i.e., with frequency to the −2 power. Figure 1 shows an example of power density spectra for three tracking levels. For this particular experiment a one-component LDV system was used at $x/d = 60$ and $y/x = 0$ and the fluid was 100 ppm PEO. When the tracking percentage is between 20 and 60, little change in the spectra is found. Above 60% the low frequencies are attenuated and the high frequencies are amplified; below 20% the entire spectrum is attenuated. On the voltage scale used in Figure 1, the mean velocity was approximately 0.17 volts (44 cm/s) and the turbulence intensity based upon the 30% tracking level was 29%. When the noise level is low, the spectra can be analyzed to distinguish the turbulence and noise.

The experiments were repeated several times with the three different types of water and no differences were found. Accuracies of the turbulent intensities were ±1% near the jet center and ±10% at $y/x = 0.1$.

RESULTS AND DISCUSSION

Flow Visualization

Photographs of the jet showing the darkened areas of india ink are shown in Figure 2. Poly(ethylene oxide) solutions in distilled

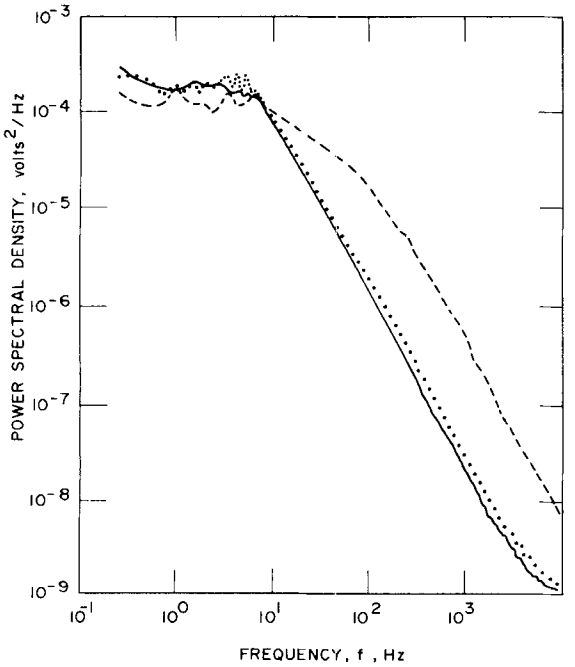

Figure 1. Effect of amplification or tracking percent on noise in LDV measurements; tracking levels: 30%, —; 55%, ·····; and 80%, - - - -.

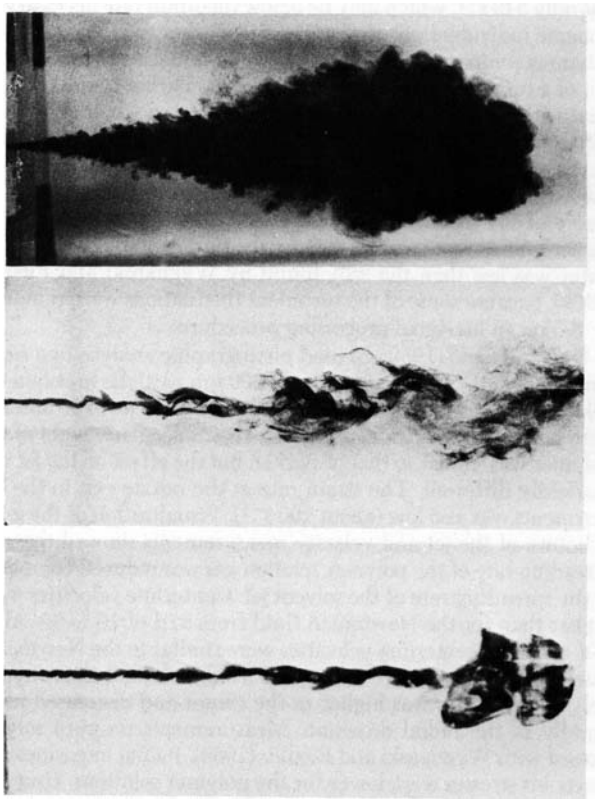

Figure 2. Photographs of jets in three fluids: top, water; middle, 100 ppm PEO in distilled water; bottom, 100 ppm PAM in deionized water.

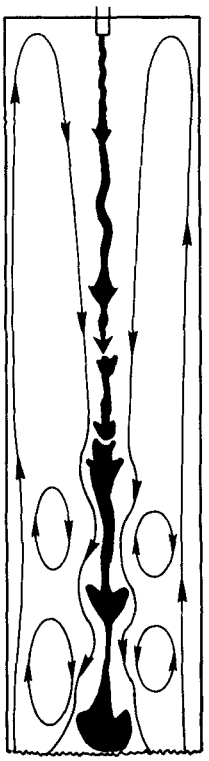

Figure 3. Drawing of jet flow pattern for 100 ppm PAM in deionized water showing reduced spread and rapid recirculating eddy.

water look quite different from a Newtonian jet. The spreading for PEO begins at a larger x distance from the nozzle, and the mixing due to small scales of turbulence appears suppressed. The PEO jet has threads oriented in the axial direction. These threads become thinner and finally disappear or mix completely after 100 jet diameters downstream. The elastic strings are regions with the same polymer concentration as the surroundings but with a different history. The PAM jet is not turbulent. Disturbances can be seen along the boundary between the colored jet and the ambient fluid. The PAM jet created a large external flow as shown in Figure 3.

Even with this secondary flow, the PAM jet does not show much mixing and the dyed fluid piles up at the bottom of the enclosure. Additional photographs of the PAM jet showed bursts of vortices and undulations of the jet occurring at intervals beginning 10 to 20 diameters from the nozzle exit. As these grew further from the nozzle they expanded the inner tube into the secondary flow. Thus we could see waves along the boundary of the flow between the inner flow and the secondary flow. It is difficult to explain the lack of mixing even on the molecular level without considering some form of network formation along with association of the water.

Mean Velocities

The mean velocity in the submerged jet decreases from the jet exit velocity to essentially zero far from the jet. This decay along the jet axis is shown in Figure 4. For water the results are similar to Wygnanski and Fiedler or the initially laminar jet of Hussain (1982). Poly(ethylene oxide) solutions of 25 ppm have no significant differences from water. At 100 ppm in tap water the PEO solution has a slightly slower rate of decay; when deionized water is the solvent, the decay rate is even slower. The 100 ppm PAM solutions have a much slower rate of decay of the mean velocity than any of the other fluids. Here we use rate of decay to compare the change in centerline velocity with axial distance from the jet.

Reynolds numbers were 10^4 and 1.4×10^4 for water, 7,500 to 8,000 for PEO solutions and 2,400 to 4,200 for PAM solutions based on viscosities measured in laminar capillary flow. As the Reynolds number is reduced the curves in Figure 4 show slower rates of decay. However, the true nozzle exit Reynolds number for the

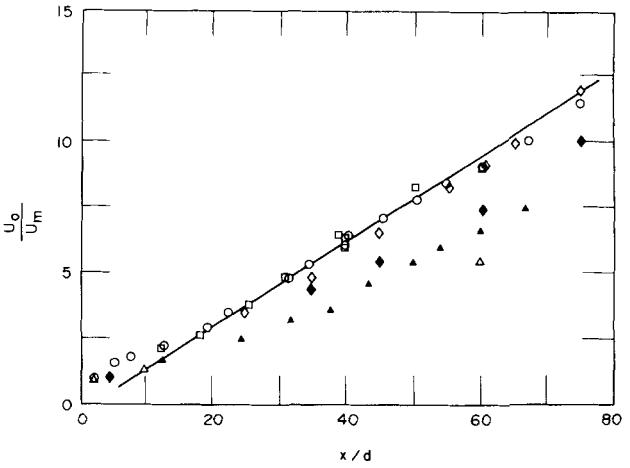

Figure 4. Jet decay as a function of downstream distance: water, ○; 25 ppm PEO in tap water, □; 100 ppm PEO in tap water, ◇; 100 ppm PEO in distilled water, ◆; 100 ppm PAM in distilled water, ▲; 100 ppm PAM in deionized water, △; the line is the initially laminar curve of Hussain (1982).

polymer solutions is not known because the solutions are shear thinning and the viscosity could vary greatly across the cross section. The jet decay data could be caused by differences in the initial formation of the jet and changes in the hypothetical origin of the jet or the effective diameter. Hussain (1982) found that the use of an effective diameter rather than the actual jet diameter did correlate the decay of initially laminar and turbulent air jets. An alternate interpretation is to consider a reduction in eddy viscosity for the polymer solution jets. A lower eddy viscosity would mean a lower slope for the curve shown in Figure 4.

Figure 5 shows the mean velocity profiles in the axial direction. The radial mean velocities were not measured because their small values close to zero had large errors. Experimental data for water was measured at x/d of 40 and 60; for 100 ppm PEO at x/d of 40 and 60; for 100 ppm PAM in distilled water at x/d of 50 and 60; and for 100 ppm PAM in deionized water at x/d of 60 only. The mean velocity profiles for water and all solutions of PEO are similar, but the PAM solutions have a much narrower velocity profile. Usui and Sano obtained velocity profiles for 200 ppm PEO which look similar to the PAM profiles here. The water results follow the turbulent profile predicted by Hinze (1975).

The jet spread rates at $x/d = 60$ in terms of the ratio of the jet half-width to x are 0.1 for the Newtonian fluid, and for the 25 ppm PEO in tap water; 0.09 to 0.1 for 100 ppm PEO; 0.07 for 100 ppm PAM in distilled water; and 0.055 for 100 ppm PAM in deionized water. For the PAM solutions the relative difference in spread rate

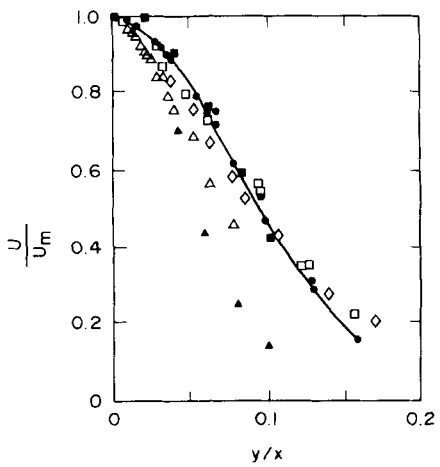

Figure 5. Velocity profiles at $x/d = 60$: water, ●; 25 ppm PEO in tap water, □; 100 ppm PEO in tap water, ◇; 100 ppm PEO in distilled water, ■; 100 ppm PAM in distilled water, △; 100 ppm PAM in deionized water, ▲; the line is the Newtonian curve of Hinze (1975).

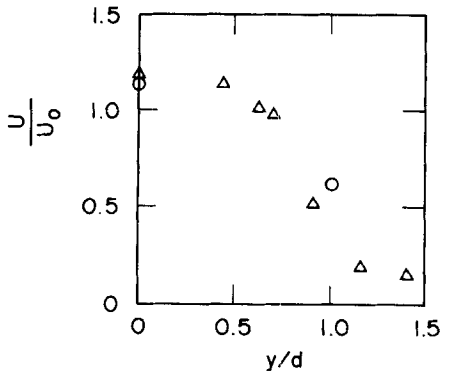

Figure 6. Velocity profile at $x/d = 2$: water, ○; PAM in deionized water, △.

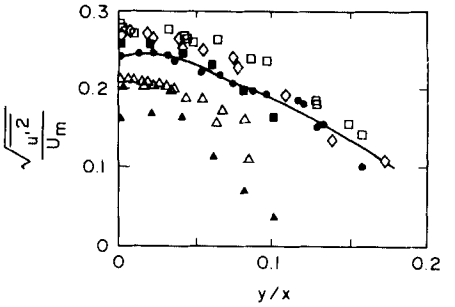

Figure 8. Intensity of u' fluctuation across the jet: water, ●; 25 ppm PEO in tap water, □; 100 ppm PEO in tap water, ◇; 100 ppm PEO in distilled water, ■; 100 ppm PAM in distilled water, △; 100 ppm PAM in deionized water, ▲; the line is drawn by eye through the points for water.

vs. the Newtonian fluid is the same as the relative difference in jet decay rate. This indicates that a change in effective diameter would bring the two sets of data together. The PEO solutions do not show equivalent changes in decay rates and spread rates.

Close to the jet nozzle at $x/d = 2$ we measured U_m/U_o of 1.2 for the PAM solution in deionized water. The velocity profile is shown in Figure 6. Two points for the water profile are also shown. We assume from these data and from the flow visualization that the jets initially were all laminar and the major difference in the fluids was in their elastic nature.

Velocity Fluctuations

The development of the axial velocity fluctuations along the jet centerline are shown in Figure 7. The water jet has a constant axial turbulent intensity of 25% of the centerline velocity after $x/d = 40$. This result is in agreement with Hussain (1982) when the jet origin is laminar. An initially turbulent jet was found to be self-preserving by Hussain with the same turbulent intensity only for x/d greater than 100. For axial distances from the nozzle exit less than this, the intensity rose to 28% at $x/d = 50$ and then declined.

The axial turbulence intensity for all the PEO solutions increased above that for the pure solvent for x/d greater than 40. When x/d was less than 40, 100 ppm PEO solutions had a lower axial intensity on the jet centerline than the Newtonian fluid. PAM solutions always had lower turbulent intensities compared to water. The increase for PEO solutions seems to correspond to the existence of the strings that were observed in the flow visualization photographs and shown in Figure 2. No strings were seen in the PAM solutions and we observe lowered turbulent fluctuations.

Further details of the axial turbulent fluctuations are shown in Figure 8. The data points are at x/d of 40 and 60 for water and 100 ppm PEO in tap water, and at x/d of 50 and 60 for PAM in distilled water. The other fluids were measured at x/d of 60 only. For water the maximum in the axial turbulent intensity occurs somewhat off of the center but the difference between the center and the maximum is small (24.3% at the center, and 24.6% at $y/x = 0.02$ for $x/d = 60$). This difference is more than the experimental uncertainty and has been observed previously (Abbiss et al., 1975). Figure 8 shows that the PEO solutions have an increased axial turbulence intensity compared to the solvent for y/x less than 0.1. PAM solutions have a reduced axial intensity of u' fluctuations and a reduced spread over which these fluctuations exist compared to the solvent.

Figure 9 shows the radial turbulent intensity as a function of radial distance from the jet center. The axial positions are the same as for Figure 8. In contrast to the increased u' fluctuations for PEO solutions, the v' fluctuations are unchanged compared to water across the jet for 25 ppm and 100 ppm in tap water. The radial turbulent intensity is decreased across the jet for 100 ppm PEO and PAM in distilled or deionized water with the extent of the decrease in the same direction as the changes in jet decay and spread rates of the mean velocities. Solvent radial turbulent intensities measured in this work are lower than those of Wygnanski and Fiedler (1969). The reductions are similar to the differences in the axial intensities; however, Wygnanski and Fiedler observed that the radial intensities took a longer axial distance to become self-preserving. Our x/d distance of 60 is probably not enough to reach self-preservation for the dilute polymer solutions where the velocity profile is narrower than the Newtonian case.

Power Spectra

Additional information on the turbulent structure can be found in the power spectra of the u' and v' fluctuations. The normalized spectra at $y/x = 0$ and $y/x = 0.05$ for $x/d = 60$ are shown in Figures 10 through 13. Only the 100 ppm PEO in tap water and 100 ppm PAM in distilled water were examined for the details of the power spectra.

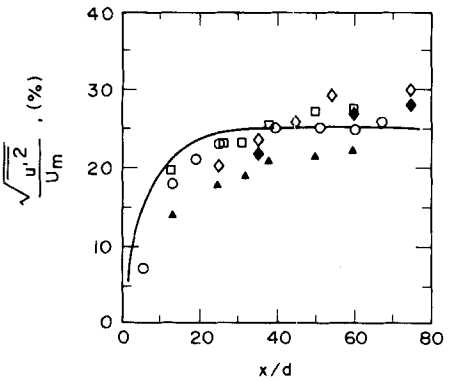

Figure 7. Development of centerline axial turbulence intensity: water, ○; 25 ppm PEO in tap water, □; 100 ppm PEO in tap water, ◇; 100 ppm PEO in distilled water, ◆; 100 ppm PAM in distilled water, ▲; the line is the curve of Hussain (1982) for the initially laminar jet.

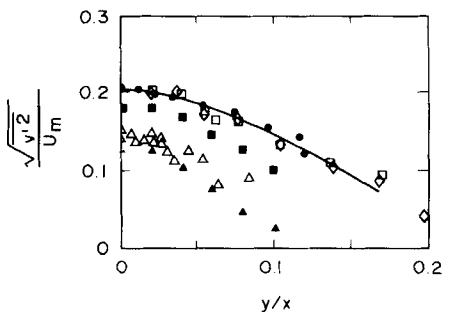

Figure 9. Intensity of v' fluctuation across the jet: water, ●; 25 ppm PEO in tap water, □; 100 ppm PEO in tap water, ◇; 100 ppm PEO in distilled water, ■; 100 ppm PAM in distilled water, △; 100 ppm PAM in deionized water, ▲; the line is drawn by eye through the experimental points for water.

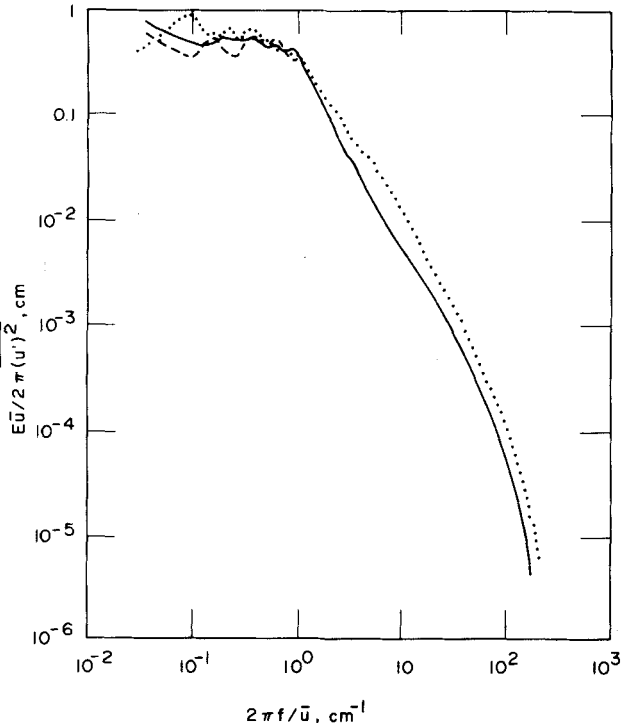

Figure 10. Power spectral densities of u' at the jet centerline $x/d = 60$: water, ·····; 100 ppm PEO in tap water, ——; 100 ppm PAM in distilled water, - - -. After $k = 1$ the curves for the two polymer solutions are the same; data were measured on-line and are corrected for turbulent ambiguity noise.

The power spectra of the axial turbulent fluctuations only show significant differences at higher wave numbers where the polymer solution results are slightly attenuated. The lateral turbulent fluctuation power spectra have differences at low and high frequencies. Again, the solvent has a higher power spectral density at high frequencies. The integral scales calculated from the lowest frequency values of the power spectra are self-preserving for all the fluids for x/d greater than 40. Our measurements show that the axial integral scales at $y/x = 0$ divided by the distance from the nozzle, Λ_f/x are 0.064 for 100 ppm PAM, 0.077 for 100 ppm PEO, and 0.072 for water. We have assumed Taylor's hypothesis in these calculations.

The ratio of the axial integral scale to the lateral scale, Λ_f/Λ_g at the jet center was 2.3 for water, 1.7 for 100 ppm PEO, and 3.8 for 100 ppm PAM. This trend is shown by the relative positions of

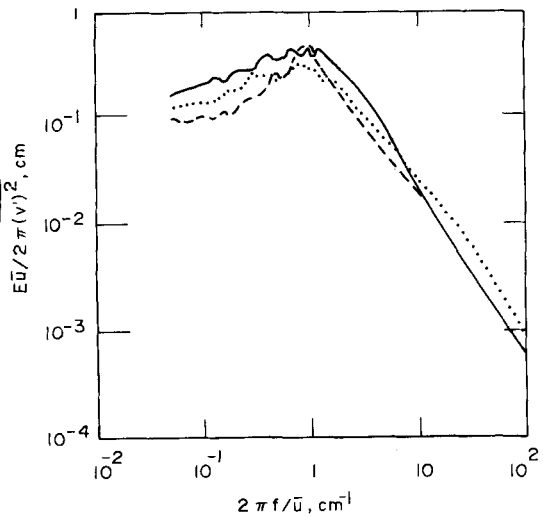

Figure 11. Power spectral densities of v' at the jet center $x/d = 60$; solutions as in Figure 10.

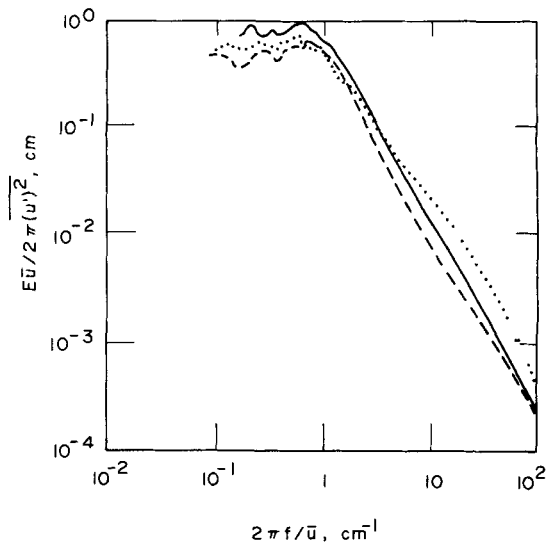

Figure 12. Power spectral densities of u' at $y/x = 0.05$ and $x/d = 60$; solutions as in Figure 10.

the power spectra at low frequencies in Figure 1. We found a small decrease in Λ_f/Λ_g as y/x increased to 0.05 for water and PEO, but an increase to 5.5 for PAM.

The implications are that the large eddies are stretched in the longitudinal direction in the case of PAM solutions. Usui and Sano (1980a) found this for their PEO solutions, and their photographs look like our PAM solutions. The large eddies would appear to be stretched in the radial direction to account for the reduced Λ_f/Λ_g for PEO in tap water, but the photographic evidence of the oriented strings in the axial direction is counter to this argument. The smaller scale in the axial direction must represent the relative motions of the elastic strands in the two directions.

The Taylor microscale λ_f at the jet center and $x/d = 60$ was calculated from the energy spectra. The Newtonian value was 1.2 mm, so the ratio λ_f/Λ_f is similar to Wygnanski and Fiedler. The polymer solution Taylor microscale is 20% higher than the Newtonian fluid. The Kolmogorov microscales were approximately 30 μm for water, 35 μm for PEO, and 50 μm for PAM. The PAM scale depends upon the viscosity used in the calculations. The differences do scale with the viscosity measured in capillary tubes and represent a change in Reynolds number of the flow. The major change in the structure for the most elastic polymer solution compared to

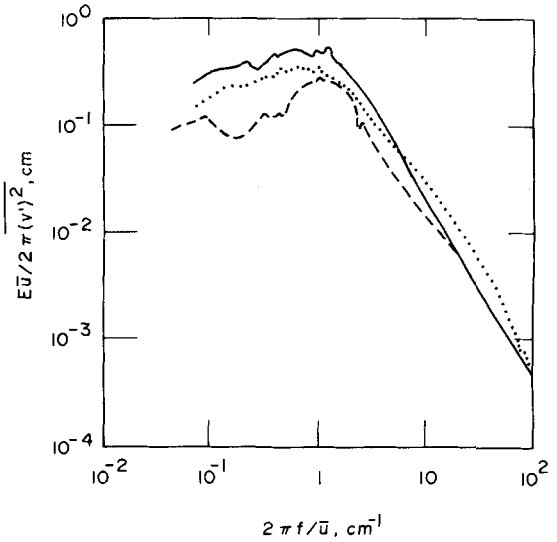

Figure 13. Power spectral densities of v' at $y/x = 0.05$ and $x/d = 60$; solutions as in Figure 10.

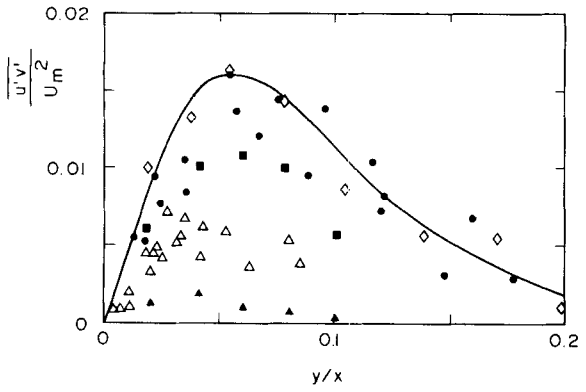

Figure 14. Shear stress distribution across the jet: water, ●; 100 ppm PEO in tap water, ◇; 100 ppm PEO in distilled water, ■; 100 ppm PAM in distilled water, △; 100 ppm PAM in deionized water, ▲; the line is computed from the mean profile for the Newtonian fluid.

the Newtonian flow is the size of the lateral integral scale. This size correlates with the reduction in the spread of the jet.

Shear Stress

Figure 14 shows the $u'v'$ correlation or Reynolds stress across the jet for the different fluids. Water closely follows the results of Wygnanski and Fiedler, with some results close to the calculated curve and some below. The polymer solutions follow the visual observations of the spreading of the jet. For 100 ppm PEO in tap water the results are similar to the solvent, but when distilled water is the solvent the turbulent stress is reduced. The $u'v'$ correlation for 100 ppm PAM solutions is sensitive to the solution preparation. We show two different curves for PAM in distilled water representing different batches. For these, little change was found in the other properties. The jet was wider for the solution corresponding to the highest curve for PAM in Figure 14. When deionized water was used, the Reynolds stress fell to very low values, indicating that the longitudinal and lateral fluctuations were not due to turbulence. Corresponding to the reduced width of the jet in PAM solutions, the peak in the $u'v'$ correlation occurred at smaller values of y/x than for water. The measurement of the $u'v'$ correlation shows that although longitudinal and lateral fluctuations are present in the polymer solutions, they do not always correlate. This type of flow may also exist in drag reduction in turbulent wall shear flows. That is, large scale fluctuations remain but they do not give turbulent diffusion.

Probability Density

The variations in skewness and flatness of the longitudinal and lateral velocity probability densities were measured. For the water, the u' and v' probability densities have similar forms and are close to the results of Wygnanski and Fiedler. The polymer solutions have a different behavior. The skewness is increased compared to the solvent for all of the polymer solutions except the PAM in deionized water. This behavior depends upon the location of the measurements compared to the large scale eddy structure and the symmetry of these structures. The flow visualization shows that the instabilities of the PAM in deionized water jet are always symmetric.

The flatness factor for y/x less than 0.1 remains close to Gaussian for all the data. There is a tendency for the flatness to increase with y/x, but the increase for a Newtonian fluid is known to occur for y/x greater than 0.1. The v' for PAM in deionized water has a slightly higher flatness than the other fluids, which indicates a larger difference between fast- and slow-moving regions in the radial direction.

SUMMARY AND CONCLUSIONS

When polymer jets differ from a Newtonian jet, photographs show that the polymer jet remains together and does not break up into turbulence very readily. The solvent jet becomes turbulent within a few jet diameters from the jet source but the polymer solution jets can have well-defined instabilities which persist for over 100 jet diameters from the source. A wide range of polymer solution effects on the jet can be observed and these affects are dependent upon the purity of the water used in the initial preparation of the solution.

The solutions of PEO in tap water showed only a small increase in axial fluctuations compared to water alone. In purified water, 100 ppm PEO jets had decreased fluctuations in the radial direction and decreased Reynolds stress compared to water alone. Further examination of the details of the fluctuations showed that the small eddies were decreased and the large scale fluctuations increased. The relative change in the large eddies was larger in the radial direction and we propose that this comes from the oscillations of the strings formed from the breakup of polymer networks. These strings are visible in photographs of the jet when india ink is added to the fluid.

PAM molecules in distilled or deionized water are expanded polyelectrolytes and the expansion is affected by small amounts of ions in the solution. Jets of 100 ppm PAM have greatly reduced mixing, compared to PEO jets. The magnitude of both the large fluctuations and the small fluctuations is reduced. For PAM, in contrast to PEO, the radial large scale is reduced much more than the axial large scale. Flow visualization shows that the fluid which has gone through the jet remains together and does not form threads. Only well-defined large eddies can be seen and no small-scale structure is visible. The fluctuations are the presence and absence of these large eddies, and little turbulent mixing occurs.

We conclude that the elastic nature of these solutions does affect the turbulent jet but the effect is complex and can result in increased or decreased fluctuations. Network bonds are broken to form the shear layer interface between high-speed jet fluid and low-speed ambient fluid but we know little about the behavior of such non-uniform viscoelastic fluids in shear layers.

ACKNOWLEDGMENT

The authors acknowledge the support of the National Science Foundation under Grant CPE 8022433.

NOTATION

d = jet diameter
E = power spectral density
f = frequency
k = $2\pi f/\bar{u}$
U_m = local centerline velocity
U_o = initial velocity assuming plug flow
u = axial velocity
$\bar{u}$ = time-averaged axial velocity
u' = axial velocity fluctuation
v = radial velocity
v' = radial velocity fluctuation
x = axial distance from origin of jet
y = radial distance from jet center
Λ_f = axial integral scale
Λ_g = radial integral scale
λ_f = axial Taylor microscale

LITERATURE CITED

Abbiss, J. B., L. J. S. Bradbury, and M. P. Wright, "Measurements on an Axi-Symmetric Jet Using a Photon Correlator," *Proc. LDA Symp.*, Copenhagen (1975).

Barker, S. J., "Laser-Doppler Measurements on a Round Turbulent Jet in Dilute Polymer Solutions," *J. Fluid Mech.*, **60**, 721 (1973).
Berman, N. S., and J. W. Dunning, "Pipe Flow Measurements of Turbulence and Ambiguity Using Laser-Doppler Velocimetry," *J. Fluid Mech.*, **61**, 289 (1973).
Chang, H. D., and R. Darby, "Effect of Shear Degradation on the Rheological Properties of Dilute Drag-Reducing Polymer Solutions," *J. Rheology*, **27**, 77 (1983).
Filipsson, L. G. R., J. H. Lagerstedt, and F. H. Bark, "A Note on the Analogous Behavior of Turbulent Jets of Dilute Polymer Solutions and Fiber Suspensions," *J. Non-Newtonian Fluid Mech.*, **3**, 97 (1977).
Hinch, E. J., and C. Elata, "Heterogeneity of Dilute Polymer Solutions," *J. Non-Newtonian Fluid Mech.*, **5**, 411 (1979).
Hinze, J. O. *Turbulence*, McGraw Hill, New York, 1975.
Hussain, Z. D., "An Experimental Study of Effects of Initial and Boundary Conditions on Near and Far Fields of Jet Flows," PhD Dissertation, Univ. Houston (May, 1982).
Metzner, A. B., and A. D. Metzner, "Stress Levels in Rapid Extensional Flows of Polymeric Fluids," *Rheol. Acta*, **9**, 174 (1970).
Usui, H., and Y. Sano, "Turbulence Structure of Submerged Jets of Dilute Polymer Solutions," *J. Chem. Eng. Japan*, **13**, 401 (1980a).
———, "Turbulent Flow Structure of Submerged Jets of Dilute Polymer Solutions," *Technical Report*, **2**, 4, Yamaguchi Univ. (1980b).
Wygnanski, I., and H. Fiedler, "Some Measurements in the Self-Preserving Jet," *J. Fluid Mech.*, **38**, 577 (1969).

Manuscript received March 11, 1983; revision received August 25, and accepted January 16.

Improved Dead-Time Compensator Controllers

It is shown that the conventional Smith dead-time compensator can be modified in a fashion which leads to significant improvements in its regulatory capabilities for measurable disturbances or inputs. The proposed modification utilizes effectively the existing prediction capabilities of the conventional dead-time compensator and eliminates the need for a separate feedforward controller in many circumstances under which it is normally employed. The modified dead-time compensator possesses simultaneous feedforward and feedback actions. An additional tuning parameter which controls the degree of dead-time cancellation allows the designer to shape the response according to requirements. Illustrative examples show the advantages of the modified scheme.

Z. J. PALMOR
Faculty of Mechanical Engineering,
Technion
Israel Institute of Technology
Haifa, Israel

D. V. POWERS
Taylor Instrument Company
Rochester, NY 14692

SCOPE

A long-standing problem in process control is that of controlling processes with significant deadtimes between inputs and outputs. A considerable improvement in the control in these cases may be obtained via the O. J. M. Smith dead-time compensator (DTC) which recently has been extended to systems with multiple dead times. While the inclusion of the DTC considerably improves the performance of the controlled loop for setpoint changes, as has been shown by numerous experimental and simulation studies, the enhancements in disturbance rejection capabilities are not as apparent.

This paper reveals the reason for this and presents a simple, yet novel, modification of the DTC. With this modification, the dead time of the system to measurable disturbances is also compensated. This leads to significant improvements in the regulation capabilities of the DTC while retaining all its other properties.

By treating the degree of compensation as a design parameter, it is shown that the overall performance may be further improved in certain cases. Analytical approach to the determination of the degree of compensation is also discussed.

The main features of the new design are demonstrated through simulated responses.

CONCLUSIONS AND SIGNIFICANCE

The servomechanism properties of process controllers are considerably improved by the inclusion of a conventional dead-time compensator. DTC-based controllers traditionally have been considered and treated as feedback-only control schemes, and therefore no attention has been paid to the possibility of extending their properties to those of feedforward controllers. The modified DTC proposed in this paper utilizes the existing process model contained in the conventional DTC to predict the effect of the disturbances on the outputs. These predictions are further used in the new DTC to cancel the long dead times that usually exist between the disturbance and its effect on the output. Consequently, the control actions taken counteract the effect of the disturbances before they can appreciably change the output. In this fashion, the conventional DTC is extended to encompass features of feedforward controllers without the employment of separate controllers. This leads to significant improvements in the regulation properties while the servomechanism properties of the conventional DTC are clearly preserved, and the sensitivity to modeling errors is unaltered.

The modified DTC is quite flexible. It is possible to design it for partial DT cancellation rather than for full cancellation. In some cases further improvement may be achieved in this fashion. The degree of cancellation may be considered as a